▌Heterogeneous Catalysis |*Very Important Paper*|

VIP
Hydrophobic Modification of Pd/SiO₂@Single-Site Mesoporous Silicas by Triethoxyfluorosilane: Enhanced Catalytic Activity and Selectivity for One-Pot Oxidation

Kazuki Nakatsuka,[a] Kohsuke Mori,[a, b] Shusuke Okada,[a] Shohei Ikurumi,[a] Takashi Kamegawa,[a, b] and Hiromi Yamashita*[a, b]

Core-shell catalyst
One-pot oxidation
Hydrophobicity

These are not the final page numbers! ↗↗
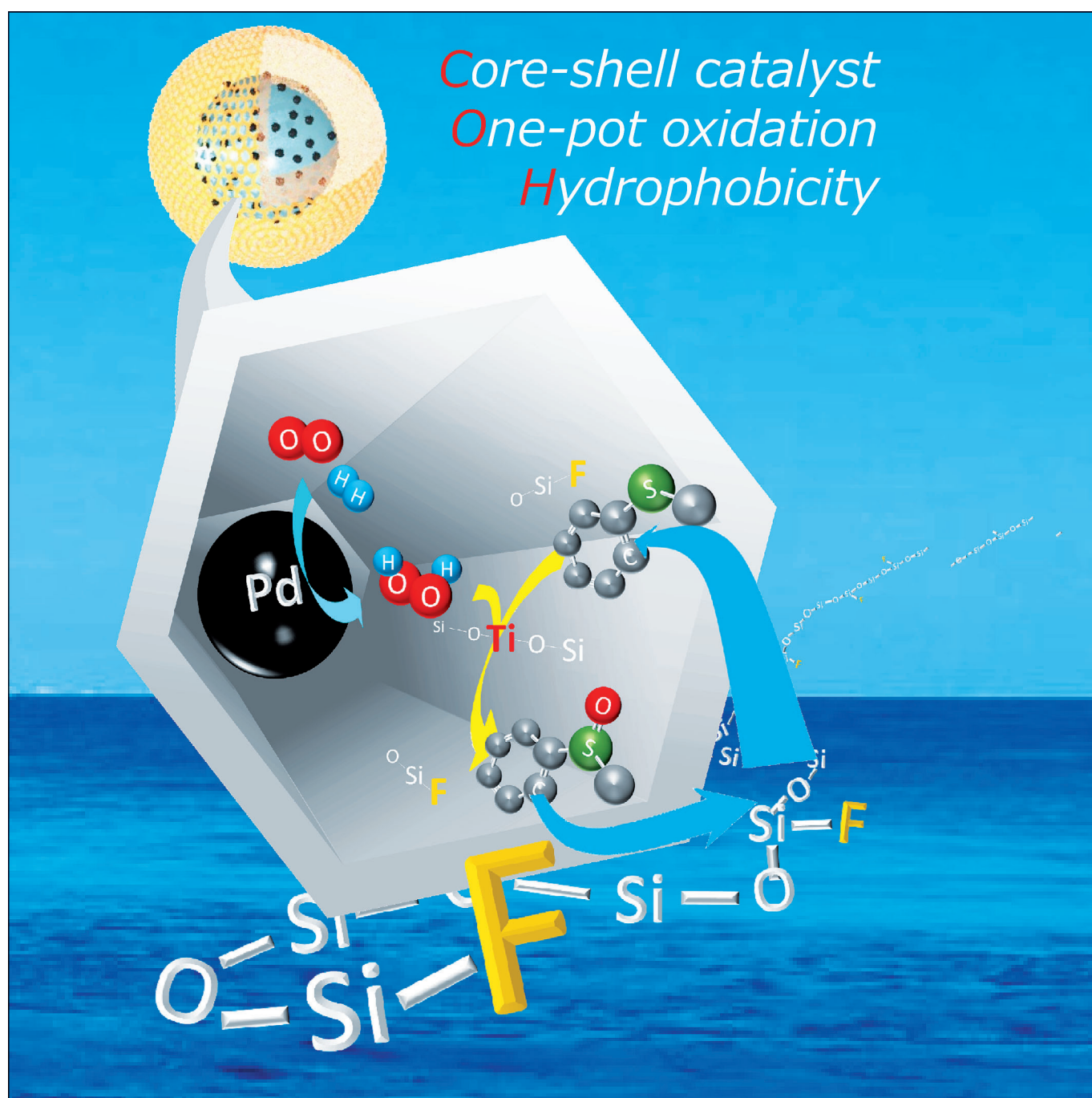
Abstract: To enhance the catalytic activity in a selective one-pot oxidation using in-situ generated H_2O_2, a hydrophobically modified core–shell catalyst was synthesized by means of a simple silylation reaction using the fluorine-containing silylation agent triethoxyfluorosilane (TEFS, $SiF(OEt)_3$). The catalyst consisted of a Pd-supported silica nanosphere and a mesoporous silica shell containing isolated Ti^{IV} and F ions bonded with silicon (Si–F bond). Structural analyses using XRD and N_2 adsorption–desorption suggested that the mesoporous structure and large surface area of the mesoporous shells were retained even after the modification. During the one-pot oxidation of sulfide, catalytic activity was enhanced significantly by increasing the amount of fluorine in the shell. A hydrophobic surface enhanced adsorption of the hydrophobic reactant into the mesopore, while the less hydrophobic oxygenated products efficiently diffused into the outside of the shell, which improved the catalytic activity and selectivity. In addition, the present methodology can be used to enhance the catalytic activity and selectivity in the one-pot oxidation of cyclohexane by using an Fe-based core–shell catalytic system.

Introduction

Hydrogen peroxide (H_2O_2) is a safe and environmentally friendly oxidizing agent. Therefore, the selective oxidation of organic compounds using H_2O_2 is of interest in the manufacturing of many fine chemicals. Commercial production of H_2O_2 is accomplished through the anthraquinone process, which involves the sequential hydrogenation and oxidation of alkyl anthraquinone. This requires toxic solvents and a large energy input because H_2O_2 is easily decomposed. An alternative process involving the direct synthesis of H_2O_2 from H_2 and O_2 on a Pd catalyst also has been reported.[1–3] However, the H_2O_2 generated sometimes undergoes simultaneous hydrogenation and/or decomposition to water due to the catalyst, which prevents the accumulation of H_2O_2.

To overcome the problems in the synthesis of H_2O_2, generating H_2O_2 in situ from H_2 and O_2 on a Pd-based catalyst followed by oxidation of organic reactants using the neighboring active site in the same reaction vessel is a promising strategy. This one-pot oxidation reaction uses the unstable H_2O_2 immediately after production without tedious isolation or purification steps.[4–8] A previous report described a highly efficient one-pot oxidation system using new core–shell catalysts with special attention paid to the precise architecture of two types of active sites. The catalyst was composed of a Pd-supported silica nanosphere core and a mesoporous silica shell containing atomically dispersed Ti or Fe sites. Hydrogen and oxygen gases can diffuse into the boundary of the core–shell structure through the mesoporous silica shell, where they generate H_2O_2 at the Pd nanoparticles. The H_2O_2 generated selectively interacts with the catalytically active single-site moieties (Ti or Fe) within the mesoporous silica (MS) shells to catalyze the oxidation of organic compounds, such as sulfide and phenol. This structure has the advantage that the H_2O_2 produced on the inner Pd site prevents its decomposition and allows it to be utilized before diffusing into the solution. The catalytic activity of $Pd/SiO_2@Ti$-MS using the core–shell material was about 20 times greater than that using the traditional catalyst (Pd-supported Ti-containing zeolite (TS-1)).[9] Systematic control of the Pd position, pore diameter, and thickness of the Ti-MS shell led to the enhancement of H_2O_2 efficiency.[10]

This report describes additional enhancement of the activity in one-pot oxidation by hydrophobic modification of the Ti-MS shell with a fluorine-containing silylation reagent, triethoxy fluorosilane (TEFS). We focus on the difference in hydrophobicity between the reactant, methyl phenyl sulfide, and the product, methyl phenyl sulfoxide.[11–13] The results demonstrate that the hydrophobic surface within the shells created by introduction of fluorine enhanced adsorption of hydrophobic reactants into the mesopores, while the products efficiently diffused to the outside of the shell due to their hydrophilicity, which improved catalytic activity and selectivity (Scheme 1).
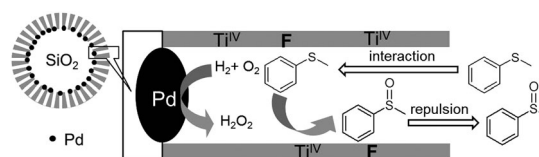
Scheme 1. Schematic illustration of one-pot oxidation of sulfide with H_2 and O_2 using $Pd/SiO_2@Ti$-MS-Fx core–shell catalyst.

Experimental Section

Materials

Tetraethoxyorthosilicate (TEOS), tetraisopropylorthotitanate (TPOT), triethoxyfluorosilane (TEFS), $SnCl_2 \cdot H_2O$, $PdCl_2$, ammonia solution (28 wt%), sodium formate, ethanol, acetonitrile, methyl phenyl sulfide, and biphenyl were purchased from Nakalai Tesque. Trimethylstearylammonium chloride (CTAC) was obtained from Wako Pure Chemical Ind. Co., Ltd.

[a] K. Nakatsuka, Prof. Dr. K. Mori, Dr. S. Okada, S. Ikurumi, Prof. Dr. T. Kamegawa, Prof. Dr. H. Yamashita
Division of Materials and Manufacturing Science
Graduate School of Engineering
Osaka University, 2-1 Yamada-oka
Suita, Osaka 565-0871 (Japan)
Fax: (+81)6-6879-7457
E-mail: yamashita@mat.eng.osaka-u.ac.jp

[b] Prof. Dr. K. Mori, Prof. Dr. T. Kamegawa, Prof. Dr. H. Yamashita
Elements Strategy Initiative for Catalysts Batteries ESICB
Kyoto University, Katsura, Kyoto 615-8520 (Japan)

Supporting information for this article is available on the WWW under http://dx.doi.org/10.1002/chem.201402586.

↖↖ **These are not the final page numbers!**

Synthesis of SiO₂ spheres

TEOS was added to a mixture of ethanol and aqueous ammonia at a TEOS/H_2O/EtOH/NH_3 molar ratio of 1:70.1:2.1:19.5. The solution was stirred for 6 h at room temperature. The product was isolated by centrifugation and washed with ethanol three times, followed by drying under vacuum at room temperature.

Synthesis of Pd/SiO₂@Ti-MS-F*x* core–shell catalyst[14]

To deposit the Pd nanoparticles onto the core, the prepared SiO_2 core (500 mg) was dispersed into water (250 mL) with ultrasonication. $SnCl_2 \cdot 2H_2O$ (500 mg) was dissolved in HCl (2×10^{-2} M, 250 mL) and the solution stirred for 10 min. This solution was added to the mixture containing the SiO_2 core. After stirring for 10 min, the suspension was centrifuged and washed with water (at least 100 mL) several times. Then the SiO_2 core containing Sn^{2+} ions was redispersed in water (240 mL) and mixed with acidic $PdCl_2$ solution (11.64 mM, 4.08 mL). After 10 min, a solution of sodium formate (0.15 M; 50 mL) was added and the resulting mixture was stirred overnight. The suspension was centrifuged and washed with water several times, to produce Pd/SiO$_2$.[15–18] To encapsulate the Pd/SiO₂ core with Ti- and F⁻-containing mesoporous silica, Pd/SiO₂ (0.5 g) was added to a mixture of ethanol (200 mL), water (150 mL), CTAC (0.71 g) and aqueous ammonia (28 wt%, 2.84 mL). After stirring for 10 min, a mixture of TEOS (for amount, see Table S1 in the Supporting Information), TEFS (for amount, Table S1 in the Supporting Information), TPOT (20.3 μL), and acetylacetone (14.1 μL) was added to the solution, which was stirred at room temperature overnight. The F/Si molar ratio in the shell was adjusted to 5, 10, 15, and 20 mol%. The catalyst referred to as Pd/SiO₂@Ti-MS-F*x* (Pd: 1 wt% against Si in the core, Ti: 2 wt% against Si in the shell) in which *x* indicates the molar ratio of F against Si in the shell. The suspension was centrifuged and washed with water (at least 100 mL) followed by drying in air for one day at 373 K. The suspension was calcined at 823 K for 6 h to remove the surfactant CTAC. The catalysts synthesized were reduced with H_2 gas before catalytic reactions.

Synthesis of Pd/SiO₂@Fe-MS-F*x* core–shell catalyst[19, 20]

To encapsulate Pd/SiO₂ within the Fe-MS shell, Pd/SiO₂ (0.5 g) was dispersed in a mixture of water (200 mL), ethanol (150 mL), CTAC (0.71 g), and ammonia aqueous (28 wt%, 2.84 mL), along with Fe-$(NO_3)_3 \cdot 9H_2O$ (13.6 mg). Then, a mixture of TEOS (750 μL: Si/Fe = 100:1 mol%) was added at room temperature and the solution stirred overnight. The dried composite was calcined at 823 K in air for 6 h to remove the CTAC structure-directing agent. The Pd/SiO₂@Fe-MS (1.0 g) was impregnated into solutions of TEFS (0.33 and 3.3 mol%) dissolved in 2-propanol (100 mL) and stirred at room temperature for 5 h. The suspension was evaporated under vacuum, dried at 373 K overnight, and then calcined at 773 K for 5 h in air.

Characterization

Powder X-ray diffraction patterns were recorded by using a Rigaku Ultima IV diffractometer with Cu$_{K\alpha}$ radiation ($\lambda = 1.5406$ Å). TEM micrographs were obtained by using a field emission-transmission electron microscope (FE-TEM; Hitachi Hf-2000) operated at 200 kV. The N_2 adsorption measurements were obtained by using a Belsorp-max system (BEL Japan, Inc.) at 77 K. The sample was degassed under vacuum at 473 K prior to data collection. The Brunauer–Emmett–Teller (BET) and Barrett–Joyner–Halenda (BJH) meth-

ods were applied to determine specific surface area and pore size distribution, respectively. The UV/Vis diffuse reflectance spectra of powdered samples were collected using a Shimadzu UV-2450 spectrophotometer. Using $BaSO_4$ as a reference, absorption spectra were obtained using the Kubelka–Munk function. Inductively coupled plasma optical emission spectrometry (ICP-OES) measurements were performed using a Nippon Jarrell-Ash ICAP-575 Mark II instrument. IR spectra were obtained as KBr pellets using a Jasco FTIR-6100 instrument. The local structures of the titanium and iron oxide species were investigated using X-ray absorption fine structure analysis (XAFS). The Ti and Fe K-edge XAFS spectra were recorded in fluorescence mode at the BL-9A facilities of the Photon Factory at the National Laboratory for High-Energy Physics, Tsukuba (2012G126). A Si(111) double crystal was used to monochromatize the X-rays from the 2.5 GeV electron storage ring. In a typical experiment, the sample was loaded into the in situ cell with plastic windows. The EXAFS data were examined using the EXAFS analysis program, Rigaku EXAFS.

One-pot oxidation of methyl phenyl sulfide

Testing catalytic reactions involving H_2 and O_2 gas safely requires special precautions. In particular, the H_2 and O_2 gas mixture should not be added directly to the dry catalyst. The catalytic reaction was conducted as follows. The catalyst (50 mg) was added to a solution of methyl phenyl sulfide (0.1 mmol), biphenyl (0.1 mmol), and acetonitrile (10 mL), fitted with a reflex condenser. The biphenyl was used as an internal standard. The mixture reacted at 303 K under a flow of H_2 and O_2 (20 mL min⁻¹, H_2/O_2 = 1:1) with stirring. The amount of product was analyzed by gas chromatography/mass spectrometry (Shimadzu GCMS-2010 plus) with TC-5HT columns.

Result and Discussion

Pd/SiO₂@Ti-MS-F*x* core–shell catalyst

The XRD patterns of all materials are shown in Figure 1. All samples had a strong diffraction peak at $2\theta = 2.0°$ associated with the d_{100} spacing, irrespective of F content, suggesting that
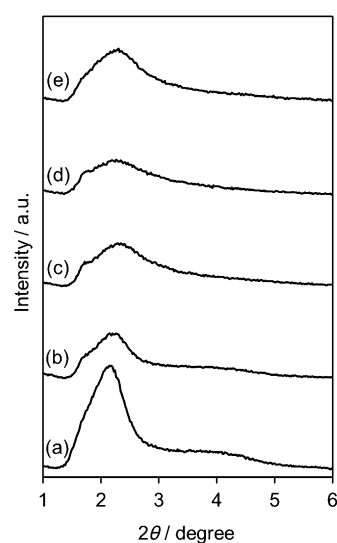
Figure 1. XRD patterns of Pd/SiO₂@Ti-MS-F*x*. F*x* = a) 0, b) 5, c) 10, d) 15, and e) 20 mol%.

These are not the final page numbers! ↗↗

the silica shell maintains ordered nanostructures. Peak intensities decreased slightly after modification, indicating that the mesostructures of the samples containing F were slightly damaged. The N_2 adsorption/desorption isotherms of each sample are shown in Figure 2. All isotherms show a typical type-IV pattern without significant hysteresis, indicating that the catalysts have a mesoporous structure. In the relative pressure range of 0.3–0.4, the isotherm exhibited a sharp inflection attributed to capillary condensation inside the mesopore at low F loading, while the inflection decreased slightly with increasing F loading. The results obtained from N_2 adsorption/desorption isotherms are summarized in Table 1. The surface areas of each sample also decreased with increased F content in the shell.
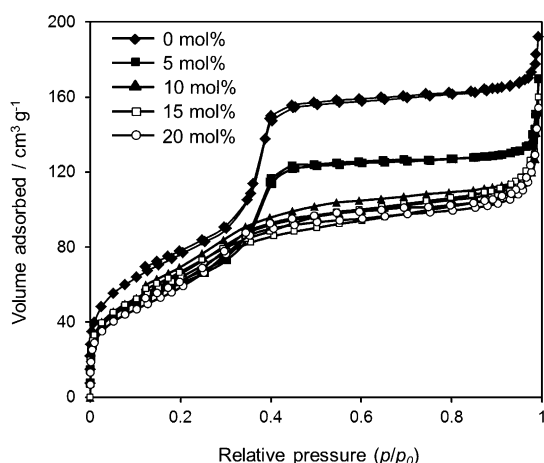

Figure 2. N_2 adsorption/desorption isotherms of Pd/SiO$_2$@Ti-MS-Fx.

Table 1. Characteristics of Pd/SiO$_2$@Ti-MS-Fx.

F content [mol%]	Pore volume [cm^3 g^{-1}]	Average pore diameter [nm]	BET surface area [m^2 g^{-1}]
0	0.29	3.10	280
5	0.25	3.16	227
10	0.21	2.60	254
15	0.24	2.26	246
20	0.21	2.60	206

The TEM images of each sample are shown in Figure 3. The synthesized SiO$_2$ particles had a spherical shape and a diameter of approximately 400 nm. The Pd nanoparticles (average diameter: 3 nm) were monodispersed and located on the boundary of the silica core surface and Ti- and F-containing mesoporous silica shells. The thickness of the mesoporous silica shells was determined to be about 40 nm for all samples. The mesoporous structure was oriented perpendicular to the core and expanded radially to the outside, which is consistent with results obtained by the XRD patterns and N_2 adsorption and desorption analyses.

Catalytic performance of the Ti-containing mesoporous silica catalyst in selective oxidation with H_2O_2 as an oxidant is affected significantly by the local structure of the Ti species. The iso-
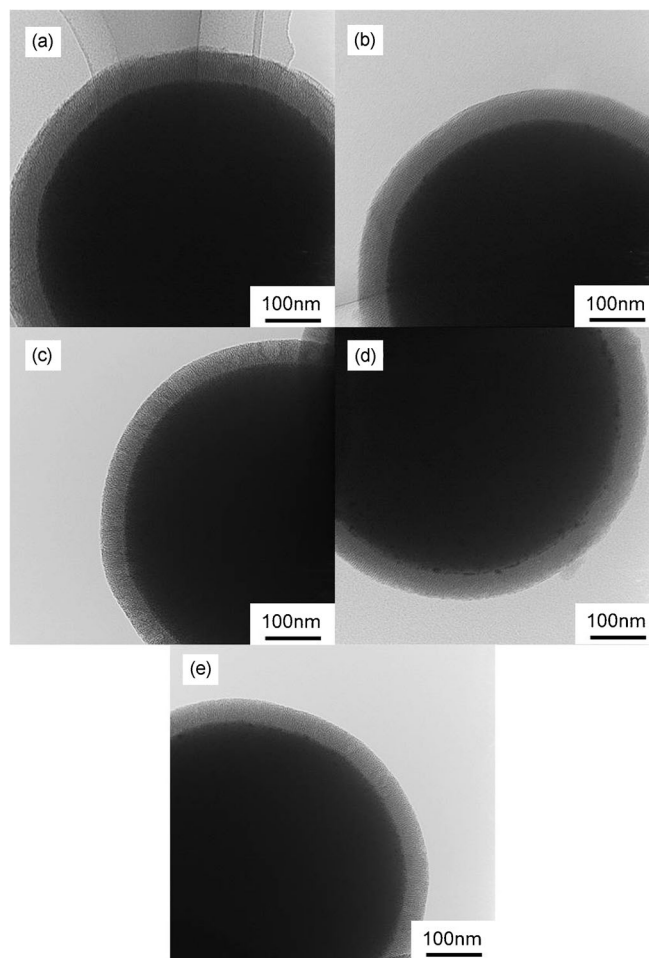

Figure 3. TEM images of Pd/SiO$_2$@Ti-MS-Fx. Fx = a) 0, b) 5, c) 10, d) 15, and e) 20 mol%.

lated tetrahedral Ti species is crucial to achieving efficient catalytic activity and selectivity. Figure 4 shows the results of Ti K-edge X-ray absorption fine structure (XAFS) analyses of Pd/SiO$_2$@Ti-MS-Fx samples, tetraisopropyl orthotitanate (TPOT, Ti(OC$_3$H$_7$)$_4$), and anatase TiO$_2$ as reference samples to investigate the local structure of Ti species contained in the shell. All of the samples with TPOT had a characteristic and sharp pre-edge peak at approximately 4970 eV, which was attributed to the transition from the 1s to 3d level of isolated tetrahedral Ti in the XANES spectra[11, 12, 21–24] (Figure 4 A). The spectrum of anatase TiO$_2$ exhibited several well-defined pre-edge peaks from 4970 to 4980 eV, which can be assigned to transitions from the 1s core level of the Ti atom to three different molecular orbitals (1t$_{1g}$, 2t$_{2g}$, and 3e$_g$) of TiO$_2$ in symmetric octahedral geometry.[13, 23, 24] The FT-EXAFS spectra are shown in Figure 4 B. The spectrum of anatase TiO$_2$ contains peaks suggestive of a contiguous Ti-O-Ti bond at approximately 2.8 Å.[13, 24] In contrast, the samples with TPOT showed only a strong peak at approximately 1.6 Å, assignable to neighboring oxygen atoms participating in a Ti—O bond.[11, 12, 21, 22, 24] In the diffuse reflectance UV/Vis (DRUV/Vis) spectra (Figure S1 in the Supporting Information), Pd/SiO$_2$@Ti-MS-Fx samples showed a ligand-to-metal charge transfer (LMCT) bond from O^{2-} to Ti^{4+} at approxi-
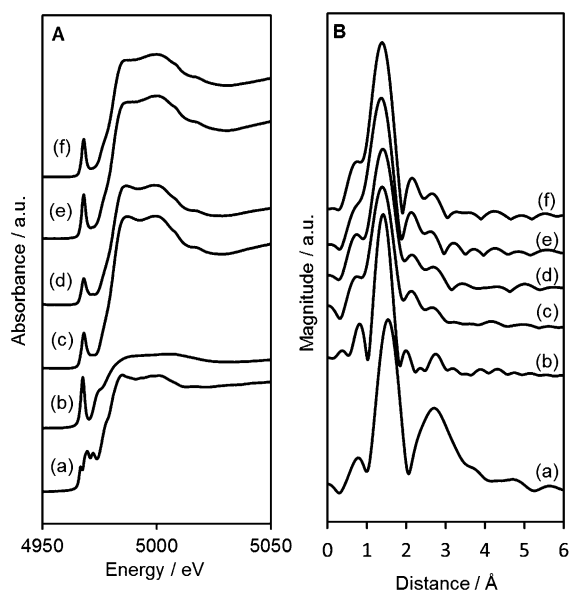
↖↖ These are not the final page numbers!

Figure 4. A) Ti K-edge XANES spectra and B) FT-EXAFS spectra of a) anatase TiO₂, b) TPOT, c) Pd/SiO₂@Ti-MS, d) Pd/SiO₂@Ti-MS-F5, e) Pd/SiO₂@Ti-MS-F15, and f) Pd/SiO₂@Ti-MS-F20.

mately 250 nm without adsorption ranging from 400 to 300 nm, suggesting the absence of extended Ti-O-Ti connectivity.[11–13] These results clearly indicate that the local coordination of Ti species in Pd/SiO₂@Ti-MS-Fx is tetrahedral, even in the presence of TEFS, and is suitable for oxidation with H₂O₂ as an oxidizing agent.

The surface properties of F-containing Pd/SiO₂@Ti-MS were evaluated using FT-IR, XPS, and H₂O adsorption. The peaks observed near 970 and 950 cm⁻¹ in the FT-IR spectra were assigned to Si–OH and Si–F stretching vibration, respectively. These peaks were very close together and appeared to be one peak. As shown in Figure S2 in the Supporting Information, the peak position shifted to shorter wavenumbers with increasing F/Si molar ratio in the shell, suggesting the appearance of Si–F bonding. In the XPS spectrum, the characteristic F species peak was present at approximately 688 eV in the F-containing Pd/SiO₂@Ti-MS (Figure S3 in the Supporting Information). Generally, F$_{1s}$ binding energy centered at 685 eV corresponds to F⁻ ions physically adsorbed onto the surface of the sample, while those centered around 688.5 eV indicate covalent F atoms, suggesting the presence of Si–F bonds in the TEFS reagent.[25,26] Both the FT-IR and XPS spectra suggested that F ions participating in Si–F bonds were introduced into the shell structure. The H₂O adsorption isotherm at room temperature is shown in Figure S4 in the Supporting Information. After surface modification, the H₂O adsorption capacity gradually decreased as the amount of F content increased, suggesting that surface hydrophobization of the shell can be achieved successfully by introduction of TEFS into the shell. The surface hydroxyl groups can act as H₂O adsorption sites because of hydrogen bonding, inducing hydrophilicity in the mesoporous materials. The decrease in the amount of H₂O adsorption can be attributed to a decrease in the number of surface hydroxyl groups

due to replacement by the TEFS reagent. To evaluate the apparent surface hydrophobicity of the surface-modified sample, toluene adsorption was measured. As shown in Figure S5 in the Supporting Information, the amount of toluene adsorbed to the F-containing mesopore in the shell was greater than that of the unmodified one. This result agrees with the results of H₂O adsorption measurements.

Evaluation of the catalytic performance was performed through one-pot oxidation of methyl phenyl sulfide (**1**) to the corresponding sulfoxide (**2**) and sulfone (**3**). Both H₂ and O₂ were indispensable for the attaining one-pot oxidation reaction. No reaction was observed when catalysts without Pd NPs or without Ti species were used. The conversion of **1** is shown in Figure 5 A. As expected, surface modification significantly improved catalytic activity compared to unmodified Pd/SiO₂@Ti-MS; the conversion of **1** increased with increasing F content in the shell, because the reactant **1** is more hydrophobic than the product, which is easily accommodated into the shell of the catalyst allowing oxidation to progress smoothly. However, the Pd/SiO₂@Ti-MS-F20 showed lower conversion than Pd/SiO₂@Ti-MS-F15, probably because some active Ti sites were covered with a large amount of TEFS and retarded the oxidation.

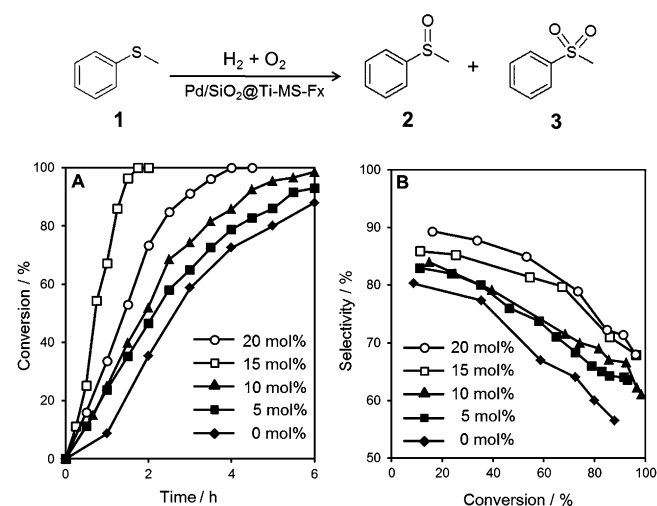**Figure 5.** A) Time course of one-pot oxidation of methyl phenyl sulfide (**1**) with H₂ and O₂ using Pd/SiO₂@Ti-MS-Fx and B) dependence of the conversion level on the selectivity of methyl phenyl sulfoxide (**2**). (Selectivity) $= [\mathbf{2}/(\mathbf{2}+\mathbf{3})] \times 100$.

Selectivities of methyl phenyl sulfoxide (**2**) toward methyl phenyl sulfone (**3**) are shown in Figure 5 B. High selectivity toward **2** was achieved by increasing the amount of F content in the shell: 90% selectivity was achieved in the presence of Pd/SiO₂@Ti-MS-F20, which was superior to the 80% selectivity obtained for Pd/SiO₂@Ti-MS. This can be attributed to the lower hydrophobicity of the product **2** compared to the reactant **1**, which subsequently diffuses to the outside, where it competes with the absorption of **1** and consequently suppresses over-oxidation of **2** to **3**. The selective oxidation of organic sulfide to sulfoxides without over-oxidation to sulfones is

These are not the final page numbers! ↗↗

a challenging goal in synthetic organic chemistry, because of the importance of sulfoxides as intermediates in biologically active compounds.[27] The present strategy using TEFS as a hydrophobizing silylation reagent provides a promising method for enhancing product selectivity. Similar phenomena also were observed for diphenyl sulfide (**4**). The greatest catalytic activity was obtained using surface-modified Pd/SiO$_2$@Ti-MS with high selectivity toward the corresponding sulfoxide **5** (Figure 6). In addition, the present catalyst can be easily separated from the reaction mixture. After the drying, the recovered catalyst was recyclable without significant loss of catalytic activity and selectivity.
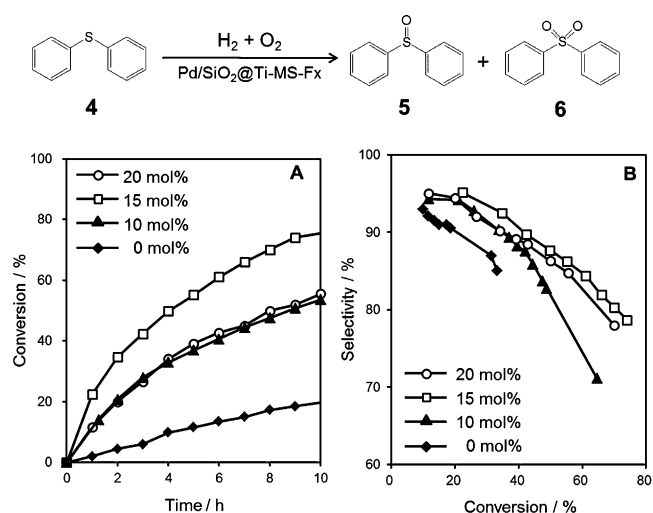
Fe-containing molecular sieves, such as Fe-containing zeolite (Fe-ZSM-5,[28] ferrisilicate[29]) and Fe-containing mesoporous silica (Fe-MCM-41,[30] Fe-MCM-48,[31] and Fe-HMS[32]) were developed, which also had high catalytic performance for oxidation reactions using H$_2$O$_2$. The isolated tetrahedral Fe is essential for selective oxidation, whereas aggregated Fe species have poor catalytic performance and undesirable H$_2$O$_2$ decomposition.[33–35] Thus, Fe K-edge XAFS measurements were performed to investigate the local structure of the Fe species together with reference compounds, ferrisilicate as isolated tetrahedral Fe and α-Fe$_2$O$_3$ as aggregated octahedral Fe species[35,36] (Figure 7). The pre-edge at about 7112 eV in the XANES spectra
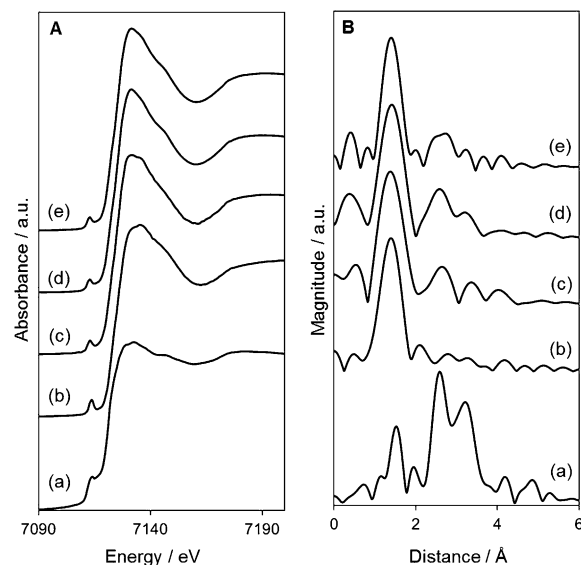

Figure 6. A) Time course of one-pot oxidation of diphenyl sulfide (**4**) with H$_2$ and O$_2$ using Pd/SiO$_2$@Ti-MS-F*x* and B) dependence of the conversion level on the selectivity of methyl phenyl sulfoxide (**5**). (Selectivity) = [**5**/(**5**+**6**)]×100.

Figure 7. A) Fe K-edge XANES spectra and B) FT-EXAFS spectra of a) α-Fe$_2$O$_3$, b) ferrisilicate, c) Pd/SiO$_2$@Fe-MS, d) Pd/SiO$_2$@Fe-MS-F1, and e) Pd/SiO$_2$@Ti-MS-F10.

Pd/SiO$_2$@Fe-MS-F*x* core–shell catalyst

This strategy, designed to enhance catalytic activity and selectivity through hydrophobitization using TEFS, was also applied to the Fe-based core–shell catalytic system. Using Fe(NO$_3$)$_2$ as an Fe source instead of TPOT allowed successful synthesis of Pd/SiO$_2$@Fe-MS (Fe: 2 wt%), Pd/SiO$_2$@Fe-MS-F1 (F/Si = 1), and Pd/SiO$_2$@Fe-MS-F10 (F/Si = 10). All samples exhibited a sharp diffraction peak centered at approximately $2\theta = 2.5°$ in the XRD pattern, which is characteristic for an ordered mesoporous structure (Figure S6 in the Supporting Information). Typical type-IV N$_2$ adsorption–desorption isotherms were observed for all samples. The BET surface area values for Pd/SiO$_2$@Fe-MS, Pd/SiO$_2$@Fe-MS-F1, and Pd/SiO$_2$@Fe-MS-F10 were 447, 200, and 198 m^{2}g^{-1}, respectively; average pore diameters as calculated by BJH method were 2.9, 1.4, and 1.4 nm respectively; and total pore volumes were 0.39, 0.12, and 0.12 cm^{3}g^{-1}, respectively. These results confirm that the mesoporous structures remained, even after modification. In the TEM images, all samples showed spherical NPs consisting of nonporous SiO$_2$ cores, Fe-containing mesoporous shells, and Pd NPs.

were attributed to the 1s–3d dipolar forbidden transition. The peak line width was very sensitive to Fe coordination number and became broader with increasing coordination number.[35,37] The pre-edge peaks of Pd/SiO$_2$@Fe-MS samples were higher than those of α-Fe$_2$O$_3$, but slightly broader than those of ferrisilicate. The Fe K-edge FT-EXAFS spectra of Pd/SiO$_2$@Fe-MS samples contained a strong peak centered at approximately 1.5 Å, which was assigned to the neighboring oxygen atoms as shown in the spectrum of ferrisilicate, accompanied by another broad peak associated with a contiguous Fe-O-Fe bond near 2.6 Å. These results suggest that the Fe species in Pd/SiO$_2$@Fe-MS exist mainly in a tetrahedral coordination, whereas some octahedral species on the extra framework of Fe-mesoporous silica also exist.

These surface-modified Fe-based core–shell catalysts also can be applied to the oxidation of cyclohexane to a mixture of cyclohexanol and cyclohexanone (Table 2). As expected, the catalytic activity was enhanced significantly by surface modification with TEFS and turnover numbers (TON) increases with increasing amounts of F in the shell. This enhanced catalytic activity also can be explained by the high hydrophobicity of

⤣⤣ These are not the final page numbers!

Table 2. One-pot oxidation of cyclohexane (**7**) with H_2 and O_2 using Pd/SiO_2@Fe-MS-F*x*.[a]

$$7 \xrightarrow[\text{Pd/SiO}_2\text{@Fe-MS-F}x]{H_2 + O_2} 8 \ (\text{OH}) + 9 \ (\text{O})$$

Sample	TON	Selectivity [%]	
		ol	one
Pd/SiO_2@Fe-MS	17	20.3	79.7
Pd/SiO_2@Fe-MS-F1	23	18.5	81.5
Pd/SiO_2@Fe-MS-F10	66	32.0	68.0

the mesoporous shell, in which hydrophobic cyclohexane was easily accommodated into the shell of the catalyst followed by oxidation. In contrast, the less hydrophobic oxygenated products, such as cyclohexanol and cyclohexanone, were removed through competition with the reactants.

Conclusion

A new core–shell type catalyst with a hydrophobic surface was designed based on a simple method using TEFS as a silylation reagent. The hydrophobic surface improved catalytic performance significantly in the one-pot oxidation of sulfides. Catalytic activity was approximately three times greater than that of previously reported unmodified catalysts, and selectivity toward sulfoxide was better due to the hydrophobic surface of the shell. This modification strategy using TEFS is a very promising method for improving the hydrophobicity of silica materials and can be used for a variety of reactions.

Acknowledgements

[1] J. M. Campos-Martin, G. Blanco-Brieva, J. L. G. Fierro, *Angew. Chem.* **2006**, *118*, 7116; *Angew. Chem. Int. Ed.* **2006**, *45*, 6962.
[2] C. Samanta, *Appl. Catal. A* **2008**, *350*, 133.
[3] S. Melada, F. Pinna, G. Strukul, S. Perathoner, G. Centi, *J. Catal.* **2006**, *237*, 213.
[4] H. Song, G. Li, X. Wang, *Microporous Mesoporous Mater.* **2009**, *120*, 346.
[5] S. K. Karmee, L. Greiner, A. Kraynov, T. E. Muller, B. Niemeijer, W. Leitner, *Chem. Commun.* **2010**, *46*, 6705.
[6] K. Mori, Y. Miura, S. Shironita, H. Yamashita, *Langmuir* **2009**, *25*, 11180.
[7] M. S. Yalfani, S. Contreras, F. Medina, J. E. Sueiras, *J. Hazard. Mater.* **2011**, *192*, 340.
[8] M. S. Yalfani, S. Contreras, J. Llorca, M. Dominguez, J. E. Sueiras, F. Medina, *Phys. Chem. Chem. Phys.* **2010**, *12*, 14673.
[9] S. Okada, K. Mori, T. Kamegawa, M. Che, H. Yamashita, *Chem. Eur. J.* **2011**, *17*, 9047.
[10] S. Okada, S. Ikurumi, T. Kamegawa, K. Mori, H. Yamashita, *J. Phys. Chem. C* **2012**, *116*, 14360.
[11] K. Ikeue, H. Yamashita, M. Anpo, T. Takewaki, *J. Phys. Chem. B* **2001**, *105*, 8350.
[12] J. Zhang, Y. Hu, M. Matsuoka, H. Yamashita, M. Minagawa, H. Hidaka, M. Anpo, *J. Phys. Chem. B* **2001**, *105*, 8395.
[13] H. Yamashita, S. Kawasaki, S. Yuan, K. Maekawa, M. Anpo, M. Matsumura, *Catal. Today* **2007**, *126*, 375.
[14] K. Chaudhari, D. Srinivas, P. Ratnasamy, *J. Catal.* **2001**, *203*, 25.
[15] K. Kaczorowska, Z. Kolarska, K. Mitka, P. Kowalski, *Tetrahedron* **2005**, *61*, 8315.
[16] A. Ungureanu, D. Trong On, E. Dumitriu, S. Kaliaguine, *Appl. Catal. A* **2003**, *254*, 203.
[17] S. Namba, A. Mochizuki, M. Kito, *Chem. Lett.* **1998**, *27*, 569.
[18] L.-S. Zhong, J.-S. Hu, Z.-M. Cui, L.-J. Wan, W.-G. Song, *Chem. Mater.* **2007**, *19*, 4557.
[19] Y. Kuwahara, K. Maki, Y. Matsumura, T. Kamegawa, K. Mori, H. Yamashita, *J. Phys. Chem. C* **2009**, *113*, 1552.
[20] Y. Kuwahara, T. Kamegawa, K. Mori, H. Yamashita, *Chem. Commun.* **2008**, 4783.
[21] H. Yamashita, S. Kawasaki, Y. Ichihashi, M. Harada, M. Takeuchi, M. Anpo, G. Stewart, M. A. Fox, C. Louis, M. Che, *J. Phys. Chem. B* **1998**, *102*, 5870.
[22] H. Yamashita, M. Honda, M. Harada, Y. Ichihashi, M. Anpo, T. Hirao, N. Itoh, N. Iwamoto, *J. Phys. Chem. B* **1998**, *102*, 10707.
[23] J. M. Thomas, G. Sankar, *Acc. Chem. Res.* **2001**, *34*, 571.
[24] K. Mori, Y. Kondo, S. Morimoto, H. Yamashita, *J. Phys. Chem. C* **2007**, *111*, 3522.
[25] J. C. Yu, J. Yu, J. Zhang, *Chem. Mater.* **2002**, *14*, 3808.
[26] D. Li, H. Haneda, S. Hishita, N. Ohashi, N. K. Labhsetwar, *J. Fluorine Chem.* **2005**, *126*, 69.
[27] R. Díaz, J. Arbiol, A. Cirera, F. Sanz, F. Peiró, A. Cornet, J. R. Morante, *Chem. Mater.* **2001**, *13*, 4362.
[28] A. L. Villa, C. A. Caro, C. M. d. Correa, *J. Mol. Catal. A* **2005**, *228*, 233.
[29] B. Li, J. Xu, J. Liu, S. Zuo, Z. Pan, Z. Wu, *J. Colloid Interface Sci.* **2012**, *366*, 114.
[30] J.-S. Choi, S.-S. Yoon, S.-H. Jang, W.-S. Ahn, *Catal. Today* **2006**, *111*, 280.
[31] W. Zhao, Y. Luo, P. Deng, Q. Li, *Catal. Lett.* **2001**, *73*, 199.
[32] H. Liu, G. Lu, Y. Guo, Y. Guo, J. Wang, *Microporous Mesoporous Mater.* **2008**, *108*, 56.
[33] C. Wu, Y. Kong, F. Gao, Y. Wu, Y. Lu, J. Wang, L. Dong, *Microporous Mesoporous Mater.* **2008**, *113*, 163.
[34] H. Liu, G. Lu, Y. Guo, Y. Guo, J. Wang, *Nanotechnology* **2006**, *17*, 997.
[35] W. Yang, Q. Zhang, T. Shishido, K. Takehira, *J. Catal.* **2002**, *209*, 186.
[36] T. Shishido, Q. Zhang, Y. Wang, T. Tanaka, K. Takehira, *Phys. Scr. T* **2005**, *2005*, 762.
[37] A. L. Roe, D. J. Schneider, R. J. Mayer, J. W. Pyrz, J. Widom, L. Que, *J. Am. Chem. Soc.* **1984**, *106*, 1676.
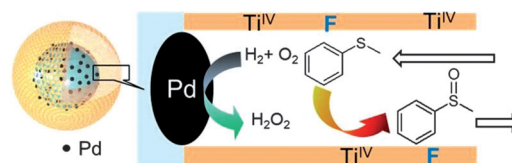
FULL PAPER

■ Heterogeneous Catalysis

K. Nakatsuka, K. Mori, S. Okada,
*S. Ikurumi, T. Kamegawa, H. Yamashita**

■■ – ■■

Hydrophobic Modification of Pd/ SiO2@Single-Site Mesoporous Silicas by Triethoxyfluorosilane: Enhanced Catalytic Activity and Selectivity for One-Pot Oxidation

Simplicity is the key: A new core–shell type catalyst with a hydrophobic surface was designed based on a simple method using triethoxyfluorosilane as a silylation reagent (see scheme). The hydrophobic surface improved catalytic performance significantly in the one-pot oxidation of sulfides. Catalytic activity was approximately three times greater than that of previously reported unmodified catalysts, and selectivity toward sulfoxide was better due to the hydrophobic surface of the shell.
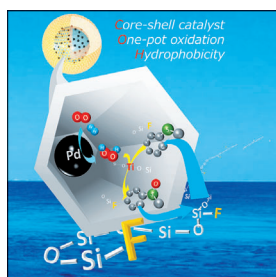
Core–Shell Catalysts

To enhance the catalytic activity in a selective one-pot oxidation using in-situ generated H_2O_2, a hydrophobically modified core–shell catalyst was synthesized by means of a simple silylation reaction using the fluorine-containing silylation agent triethoxyfluorosilane (TEFS, $SiF(OEt)_3$). For more details see the Full paper by H. Yamashita on page ■ ■ ff.

◤◤ These are not the final page numbers!